Renewable and Sustainable Energy Reviews 16 (2012) 1577–1587

Contents lists available at SciVerse ScienceDirect

Renewable and Sustainable Energy Reviews

journal homepage: www.elsevier.com/locate/rser

# A comprehensive method for optimal power management and design of hybrid RES-based autonomous energy systems

S. Abedi[a], A. Alimardani[b,*], G.B. Gharehpetian[b], G.H. Riahy[a], S.H. Hosseinian[b]

[a] Renewable Energy Lab, National Center of Excellence in Power Engineering, Department of Electrical Engineering, Amirkabir University of Technology (Tehran Polytechnic), P.O. Box: 15875-4413, 424 Hafez Ave., Tehran, Iran

[b] National Center of Excellence in Power Engineering, Department of Electrical Engineering, Amirkabir University of Technology (Tehran Polytechnic), P.O. Box: 15875-4413, 424 Hafez Ave., Tehran, Iran

ARTICLE INFO

*Article history:*
Received 22 May 2011
Accepted 25 November 2011
Available online 18 January 2012

*Keywords:*
Hybrid energy systems
Optimum power management strategy
Differential evolution algorithm
Fuzzy multi-objective optimization
Resource uncertainty

ABSTRACT

The power management strategy (PMS) plays an important role in the optimum design and efficient utilization of hybrid energy systems. The power available from hybrid systems and the overall lifetime of system components are highly affected by PMS. This paper presents a novel method for the determination of the optimum PMS of hybrid energy systems including various generators and storage units. The PMS optimization is integrated with the sizing procedure of the hybrid system. The method is tested on a system with several widely used generators in off-grid systems, including wind turbines, PV panels, fuel cells, electrolyzers, hydrogen tanks, batteries, and diesel generators. The aim of the optimization problem is to simultaneously minimize the overall cost of the system, unmet load, and fuel emission considering the uncertainties associated with renewable energy sources (RES). These uncertainties are modeled by using various possible scenarios for wind speed and solar irradiation based on Weibull and Beta probability distribution functions (PDF), respectively. The differential evolution algorithm (DEA) accompanied with fuzzy technique is used to handle the mixed-integer nonlinear multi-objective optimization problem. The optimum solution, including design parameters of system components and the monthly PMS parameters adapting climatic changes during a year, are obtained. Considering operating limitations of system devices, the parameters characterize the priority and share of each storage component for serving the deficit energy or storing surplus energy both resulted from the mismatch of power between load and generation. In order to have efficient power exploitation from RES, the optimum monthly tilt angles of PV panels and the optimum tower height for wind turbines are calculated. Numerical results are compared with the results of optimal sizing assuming pre-defined PMS without using the proposed power management optimization method. The comparative results present the efficacy and capability of the proposed method for hybrid energy systems.



## 1. Introduction

Distributed generation (DG) has been recently nominated as one of the solutions to reliable, less costly, and more efficient energy supply systems. Specifically, small DG systems with power level ranging from 1 kW to 10 MW [1], located near the loads, are extensively utilized both in grid-connected and stand-alone modes. Among available DGs, renewable-based systems (RES) such as photovoltaics and wind turbines have attained the most popularity due to ever increasing concerns about depletion of fossil fuels and global warming. They have also been getting more cost-effective during recent years.

However, a significant drawback associated with solar and wind energy systems is their intermittent and unpredictable behavior due to their direct dependence on climatic conditions. In addition, the variations of the wind and solar energy may not match with load changes [2]. The reliability of the system is important to both planning and utilization stages. Designing energy systems including solar and wind energies together, to some extent, reduces the depth of the problem. Since, the advantage of one source can overcome the disadvantage of the other one and vice versa [3]. In addition, taking into account the intermittency and uncertainty associated with solar and wind energy sources, improves the adaptation of design results with practical and realistic conditions. Another conventional solution is appropriate incorporation of energy storage devices such as batteries and hydrogen storage systems comprising electrolyzers, hydrogen tanks and fuel cells into the system [3]. Hence, hybrid energy systems are becoming more attractive to power engineers.

One of the most prominent issues regarding hybrid energy systems is to determine their optimum design and operation modes taking account of regional conditions and load demand

* Corresponding author.
*E-mail address:* arash.alimardani@ieee.org (A. Alimardani).

1364-0321/$ – see front matter © 2011 Elsevier Ltd. All rights reserved.
doi:10.1016/j.rser.2011.11.030

characteristics. Therefore, many efforts have been made for designing and planning hybrid DG systems [1–18]. These works can be reviewed from various points of view such as system modeling, the applied data in the solution algorithm, objective functions to be optimized and the mathematical tool used to handle the optimization problem. In [2], the overall cost of the introduced hybrid system throughout the estimated lifespan of the installation has been minimized. The reliability of serving energy and proper functioning of components has been involved in the applied algorithm as a constant constraint not to be violated. Solar radiation and wind speed are also assumed deterministic. Particle Swarm Optimization (PSO) algorithm has been applied to handle the single-objective problem. In [3], the cost analysis of a hybrid wind/PV/fuel cell system has been focused on through a residential consumer case study.

In [4–10], the cost has been minimized by selecting the corresponding system configuration and/or operation strategy. The load demand has been supposed to be completely or partially fulfilled with a fixed user-defined value for unmet load. In this case, the solution method has no choice to reach a compromise between cost and unmet load. In [9,10], pollutant emissions have been represented in the form of cost and limited by being economically involved in the cost function, and thus the results depend on the cost coefficient assigned to the emissions. More realistic optimal configuration may be achieved by involving pollutant emissions measurement in their relative unit (kg per liters of fuel) instead of converting it to the cost. From the aspect of the system modeling accuracy, Ref. [5], has taken a fixed PV panels tilt angle into account using Hay and Devis (1980) and Orgin and Holland (1977) methods, whereas [6] has imported the angle value as an optimization variable in the solution algorithm. In the latter work, commercially available types for each device and their costs have been taken into account, and optimization results representing size and type of each device have been demonstrated. The load demand has been assumed to be entirely fulfilled. The maximum power point tracker (MPPT) has been included in both PV and wind turbines systems. The presented approach in [7] has considered the influence of the uncertainty in solar irradiation on the sizing process of an off-shore PV power system using three probabilistic models such as Markov Chain. A size optimization procedure has been demonstrated in [8], where the results have been compared by using the optimization software called HOMER [19]. It has been stated that because of the nonlinearity and complexity of hybrid systems, the application of evolutionary algorithms like genetic algorithm generates better results than the application of classical optimization methods [8].

On the case of PMS [5], as one of the earliest works, has introduced two parameters named SDM and SAR, representing the minimum and maximum State of Charge (SOC) of batteries, respectively. The optimum values of the SOCs have been calculated within the context of the size optimization problem. Although [6] has applied an accurate model for PV and wind turbines systems representing installation parameters, the operation control has been fixedly defined by the user and did not conform with the system conditions. In [8], the effect of the minimum and maximum limit of SOC on the system operation and cost has been evaluated. The algorithm suffers a computation burden since a sub-algorithm for finding optimum values of control parameters has been executed for any single control vector generated in the main optimization algorithm as a nested optimization loop.

In [9], a grid-connected hybrid energy system, capable of mutual exchange of power with the grid, comprising wind turbine, micro-turbine, diesel generator, photovoltaic array, fuel cell and battery storage has been analyzed and on-line optimal power management has been attained. The problem has been treated as a single objective problem considering all objectives such as fuel emissions in terms of cost. The fuel emission has been factorized into three main gas components and values for each gas has been separately presented.

The cost minimization of a hybrid energy system including hydrogen storage has been presented in [10]. Using the classic linear programming optimization tool, a comparison between an optimized dispatch strategy and a fixed one has been performed so that the latter strategy can be reformed using the values obtained for the dispatch variables of the former one. Ref. [11] has incorporated the effect of the number of battery charge/discharge cycles relative to their depth of discharge (DOD) on their lifespan, operation strategy and consequently the system cost. A similar work has been addressed in [12], which has modeled the uncertainty involved in operating and design characteristics of the system taking the advantage of Stochastic Annealing optimization algorithm. This work has referenced the classification of uncertainties presented in [13] as model-inherent, system inherent and external uncertainties existing in the system.

In [14], a method has been introduced, in which the optimized configuration and operation of the system has been achieved based on twelve parameters defined relative to operational limits of different storage devices. This work has been rearranged in [15] considering a more complex hybrid system and a couple of objective functions including cost, emission and unmet load.

As seen in [14], the power available from such systems and the overall lifetime of system components are highly affected by the applied power management strategy; hence, various strategies result in various designs for the system aiming to meet load requirements within the estimated lifespan of the system.

In this work, a general method for optimal PMS of autonomous systems including various generators and storage media, combined with optimal design of system components is proposed. To do so, appropriate model of system components for the planning problem is reviewed. To solve the introduced problem, the differential evolution algorithm (DEA), which is nominated to be capable of solving various nonlinear optimization problems, is utilized. The algorithm is accompanied with the fuzzy technique to handle the multi-objective optimization problem in a time efficient manner. In this case, there is no need to find appropriate coefficients as penalty factors of constraints violations and as objective function weights. A novel method, involved in the size optimization problem, is proposed to obtain values for the parameters of PMS by which the optimum performance and minimum cost, emission and unmet load are achieved. Considering operating limitations of system devices, these parameters characterize the priority and share of each storage component for serving the deficit energy or storing surplus energy both resulted from the mismatch of power between load and RES. Optimal values for design parameters and PMS parameters are simultaneously attained.

The RES uncertainties are applied to the optimization procedure by scenario generation based on Weibull [20] and Beta distribution functions for wind speed and solar irradiation, respectively [21]. Numerical results, including type and number of each component, monthly values for PV panels tilt angle, the height of wind turbine towers along with the PMS parameters ensure the capability of the proposed method to achieve the aim of optimization. In order to focus on the significance of PMS and show the influence of strategy variations on the performance and objectives of the system, a comparison is presented, too. In addition, determining the PMS parameters in the optimization procedure is confirmed as an efficacious concept.

In the next section, the description of the system under study and the model of components are presented. Section 3 illustrates the problem statement including objective functions, constraints and the proposed method for the power management. In Section 4, DEA and fuzzy multi-objective technique are explained. Finally,

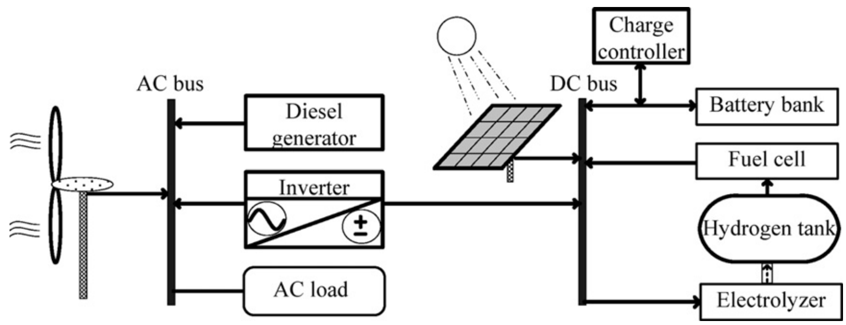



**Fig. 1.** Configuration of stand-alone hybrid energy system under study.

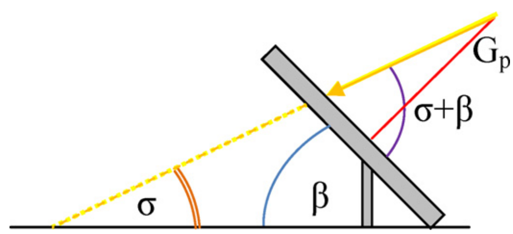



**Fig. 2.** Representation of solar elevation angle and PV panel tilt angle.

the results and conclusions are represented in two subsequent sections.

## 2. Model of system components

In this work, a stand-alone hybrid energy system comprising wind turbines, PV panels, fuel cells, electrolyzers, hydrogen tanks, batteries and diesel generators is studied. A simplified diagram of the system is depicted in Fig. 1. The available power from renewable sources is directly delivered to the load in order to provide the load demand. The excess or deficient power from RES is saved in or supplied from other equipments in the system based on the proposed dispatch strategy explained in Section 3.2. The model of each system component is briefly described in the following subsections.

### 2.1. Wind turbine

The output power of the wind turbine, $P_w$, is calculated on the basis of its power curve given by the manufacturer. The effect of the wind turbine installation height and the roughness of the land surface of the towers on the output power is also considered [2,6].

### 2.2. PV panel

To achieve the maximum output power from a PV panel, it is essential to consider the influence of the solar position and panel tilt angle. In [16], it is shown that such effects can change the total available power up to 9.94% of the total maximum power. The panels are assumed to have rotation on one axis. The following equations lead to the incident irradiation on a tilted panel. Eq. (1) is employed to calculate the longitude at the equator ($\delta$), with respect to solar ecliptic longitude and latitude ($\lambda$, $\theta$) and earth's axis inclination to the plane of its orbit ($I$ = 23.439°).

$$\delta = \sin^{-1}(\sin\ \theta \cos I + \cos\theta \sin\lambda \sin I) \tag{1}$$

The solar elevation angle ($\sigma$), which is the angle between the direction of the sun and the horizon is then estimated, as follows:

$$\sigma = \sin^{-1}[\sin\varphi \sin\delta + \cos\varphi \cos\delta \cos(\mathrm{LMST} - \lambda)] \tag{2}$$

where LMST stands for Local Mean Sidereal Time and $\varphi$ is the geography of the longitude [17]. The diffuse and reflected radiations are neglected. Using Fig. 2, the incident radiation on the tilted surface ($G_i$) can be expressed in terms of horizontal component of solar irradiation ($G_h$), as follows:

$$G_i = \frac{G_h}{\sin\ \sigma} \tag{3}$$

$$G_p = G_i \sin(\sigma + \beta) \tag{4}$$

where $G_p$ is the effective component of the solar radiation perpendicular to the panel. Based on the calculated $G_p$, the power available from PV panels at time step $t$ considering the temperature effect is determined using the following equations:

$$T_C(t) = T_A(t) + \frac{\mathrm{NCOT} - 20}{800} G_p(t, \beta) \tag{5}$$

$$I_{SC}(t) = [I_{SC,STC} + K_I(T_C(t) - 25^\circ)]\frac{G_p(t)}{1000} \tag{6}$$

$$V_{OC}(t) = V_{OC,STC} - K_V \cdot T_C(t) \tag{7}$$

$$P_M(t) = N_s \cdot N_p \cdot V_{OC} \cdot I_{SC}(t) \cdot FF(t) \tag{8}$$

where NCOT is the nominal cell operating temperature (°C), $T_A(t)$ is the ambient temperature at $t$, $T_C(t)$ is the cell temperature at $t$, $V_{OC,STC}$ and $I_{SC,STC}$ are the module open-circuit voltage and short-circuit current under STC, with $K_I$ and $K_V$ as their corresponding temperature coefficients; $P_M(t)$ is the power of array with $N_P$ modules in parallel and $N_s$ modules in series and $FF(t)$ is the fill factor [6].

### 2.3. Fuel cell

The formulations, which represent the balance between the hydrogen as input and the electric power as output in steady state condition, is the required fuel cell model used in the design procedure. However, for the sake of ensuring maximal efficiency of the system and preventing degradation of fuel cells due to abundance of start-up and shut-down cycles, a hysteresis band is also embedded into the model, as in [12].

The fuel cell hydrogen consumption, $\mathrm{Cons}_{FC}$ (kg/h), relative to its output electric power is computed by the following equation [15]:

$$\mathrm{Cons}_{FC} = \begin{cases} B_{FC} \cdot P_{N_FC} + A_{FC} \cdot P_{FC} & \text{for } P/P_{N_FC} \le P_{\max_ef} \\ B_{FC} \cdot P_{N_FC} + A_{FC} \cdot P_{FC}\left(1 + F_{ef}\left(\dfrac{P}{P_{N_FC}} - P_{\max_ef}\right)\right) & \text{otherwise} \end{cases} \tag{9}$$

where $P_{FC}$ is the output power of fuel cell in kW, $P_{N_FC}$ is the nominal output power, $A_{FC}$ and $B_{FC}$ (kg/kWh) are the coefficients of the

consumption curve. $P_{\max_ef}$, in terms of percentage of $P_{N_FC}$, is the output power, at which the efficiency of the fuel cell is maximum and $F_{ef}$ is a factor to consider the high consumption above $P_{\max_ef}$. The hydrogen consumption parameters for all fuel cells are assumed to be $A_{FC}$ = 0.05 and $B_{FC}$ = 0.004 kg/kWh, $P_{\max_ef}$ = 0.2 and $F_{ef}$ = 1 [15]. By using these values, the fuel cell efficiency is 46% at the maximum and 31% at rated powers.

### 2.4. Electrolyzer and hydrogen tank

The input electrical energy dependence on the hydrogen mass flow is modeled, as follows [15]:

$$\mathrm{Cons}_E = B_E \cdot Q_{N_E} + A_E \cdot Q \tag{10}$$

where $Q_{N_E}$ is the nominal hydrogen mass flow (kg/h), $Q$ is the hydrogen mass flow (kg/h), $A_E$ and $B_E$ are the coefficients of the consumption curve in kW/kg/h. The parameters of the electrical energy consumption for all electrolyzers are assumed to be the same as parameters given in [15], i.e., $A_E$ = 40 and $B_E$ = 20 both in kW/kg/h.

The maximum hydrogen tank capacity is assumed to be equal to 10 kg and the total capacity of the hydrogen storage is determined by the design program as the number of hydrogen tanks ($N_{tank}$). The minimum allowed level of the hydrogen (in tanks) is also a parameter determined by the proposed PMS.

### 2.5. Battery

The battery bank with the total nominal capacity of $C_n$ (Ah), can serve energy to the load until the maximum depth of discharge (DOD) or $SOC_{\min}$ is reached. $SOC_{\min}$ of battery bank along with $SOC_{\max}$ are taken into account as two of the parameters of PMS, which should be optimized by the developed program and should not exceed the values introduced by the manufacturer.

The $SOC$ of battery bank, in each simulation time step, is calculated by applying the following equation:

$$SOC(t) = SOC(t-1) + n_B \frac{P_B(t)}{C_n} \cdot 100 \tag{11}$$

where $SOC(t)$ is the batteries' $SOC$ at time step $t$, $n_B$ is the battery round-trip efficiency and $P_B(t)$ is the power charged in or discharged from battery bank at time step $t$ [6]. $n_B$ is approximately equal to 80% in charging and 100% in discharging modes [6]. $P_B(t)$ is determined due to the mismatch of power between load and RES and the share associated with batteries to supply the deficient power or to save the excess power. The mentioned share is a parameter of PMS and optimized in the proposed algorithm.

The number of series connected batteries depends on the DC bus voltage ($V_{BUS}$) and the nominal voltage of each battery, i.e.:

$$n_B^S = \frac{V_{BUS}}{V_B} \tag{12}$$

The total number of batteries in battery bank is equal to $n_B^S$ multiplied by $n_B^P$ (the number of batteries in parallel), which should be determined in the optimization algorithm.

In order to model the effect of the number of charge/discharge cycles on the lifetime of batteries, the model used in HOMER software [22] is used. This model is based on the battery "cycles to failure" curve, which is more explained in detail in [11].

### 2.6. Diesel generator

The fuel consumption of the diesel generator, $\mathrm{Cons}_G$, in terms of its output power is written, as follows:

$$\mathrm{Cons}_G = B_G \cdot P_{N_G} + A_G \cdot P_G \tag{13}$$

where $A_G$ and $B_G$ (l/kW) are fuel consumption curve coefficients provided by the manufacturer, $P_G$ (kW) is the output power and $P_{N_G}$ (kW) is the nominal output power of the diesel generator.

The values assigned to $A_G$ and $B_G$ are 0.246 and 0.08145 l/kWh, respectively, for all diesel generators, which have been used in [15], too.

## 3. Problem statement

### 3.1. Objective functions and constraints

The objective functions, considered in the optimization problem, are as follows:

- The overall cost of the system discounted to the year of installation (NPC) including the investment cost, operation and maintenance cost during the lifespan of the system, replacement cost, and fuel cost of diesel generators. All of the cost terms associated with the system components are based on the data in [15].
- The total fuel emissions produced by diesel generators during the total lifespan of the system. Thanks to the employed fuzzy multi-objective optimization technique, the model implemented for the fuel emission is adequately accurate and there is no requirement for taking it into account in terms of cost. As the most significant gas existing in the diesel generator exhaust is $CO_2$, which also causes green house effects, the produced $CO_2$ is considered to represent the fuel emission.
- The total Loss of Load Probability (*LPSP*), which represents the total unmet energy. This index is the most commonly used index in related works [2]. *LPSP* is proportional to the unmet load and is written, as follows:

$$LPSP = \frac{LOEE}{\sum_{h-1}^{H} D(h)} \tag{14}$$

where $D(h)$ is the load demand in kWh at time step $h$, and $LOEE$, standing for Loss of Energy Expected, is defined by the following equation:

$$LOEE = \sum_{h=1}^{H} E[LOE(h)] \tag{15}$$

$$E[LOE] = \sum_{s \in S} Q(s) \cdot f(s) \tag{16}$$

where $Q(s)$ represents the amount of the unmet energy when the system experiences the state $s$ and $f(s)$ is the probability associated with the occurrence of the state $s$.

The control variables, which should be used in simulations to calculate the objective functions, as well as their boundaries, are listed, as follows:

- A $k \times 2$ matrix [[$N_k$], [$T_k$]] of size parameters of the system components shown in Fig. 1, where, $N_k$ is the number and $T_k$ is the type of component $k$. Both are positive integers.
- A vector of installation parameters including monthly tilt angles of PV panels ($0^\circ < \beta_k < 90^\circ$, $k$ = 1,. . .,12) and wind turbine tower height ($h > 0$),
- A vector of PMS parameters (described in the coming section) including:
  - Monthly charge shares associated with $n-1$ types of storage media ($0 \le CS_i \le 1$, where, $n$ is the total types of the storage media existing in the system),
  - Monthly discharge shares associated with $m-1$ types of backup devices ($0 \le DS_i \le 1$, where, $m$ is the total number of backup devices capable of feeding power to the load),

- Upper and lower limits on the stored energy level of all the storage media ($SOC_{i,\min,rated} \leq SOC_{i,\min} \leq 0.5$, $0.5 \leq SOC_{i,\max} \leq SOC_{i,\max,rated}$, $0 \leq SOC \leq 1$).

In addition to the boundaries that control variables should not take values beyond them, there are operational constraints to be mentioned as follows:

- The specified maximum and minimum *SOC* of batteries ($SOC_{\min}$, $SOC_{\max}$),
- The rated current or power of all devices,
- The minimum power injected to the electrolyzers and the minimum supplied power from fuel cells and diesel generators, at which they can start-up. This constraint is considered to avoid the multitude of the start-up/shut-down cycles or short periods of frequent utilization of these devices, and enhance their lifetime. This operation limit has been introduced as Hysteresis Band Range (HBR) in [12]. Other imposed constraints are illustrated in the next section.

### 3.2. Proposed method for power management of system

In general, the PMS is so important that the operation, reliability, cost and lifetime of the system is affected with even minor alterations in the strategy. In the proposed dispatch strategy, to efficiently utilize the RES, the available power from RES, i.e., $P_{RES}(t)$, is directly delivered to the load in order to provide the load demand, $P_{load}(t)$. Other equipments are considered without any predefined priorities and there is not any preference to some components. The priorities are determined by the optimization process. The excess or deficient power of RES, i.e., $P_{rem}(t)$, is saved in or supplied from other equipments in the system, i.e.:

$$P_{rem}(t) = P_{RES}(t) - P_{load}(t) \tag{17}$$

where $P_{rem}(t)$ might be a negative or positive value.

For $P_{rem}(t) > 0$: In this case, $P_{RES}(t)$ is more than the load demand at time step *t*, and the remaining power should be delivered to the storage devices namely electrolyzers and battery bank. Therefore, based on the proposed method, the optimization procedure should assign Charge Shares (*CS*) for battery bank and electrolyzers so that $P_{rem}(t)$ is optimally shared among them considering constraints. The power, to be stored in storage device *I*, i.e., $P_i(t)$, is written, as follows:

$$P_i(t) = CS_i(k) \cdot P_{rem}(t) \quad i = 1, \ldots, n \tag{18}$$

where *n* is the total number of storage media and $CS_i(k)$ is the *CS* of storage device *i* in month *k* (*k* = 1,. . .,12). It should be mentioned that all *CSs* fall within the range (0,1).

Now, the status of all storage devices is checked one after another (as seen in Fig. 3), considering their constraints and limitations on the storable power. If any constraint is violated, $P_i(t)$ of the device should be modified so that the violated constraint is satisfied. These constraints violations or incompatibilities and the necessary modification to $P_i(t)$ in each case are, as follows:

Case (1-1): The power assigned to device *i*, $P_i(t)$, exceeds its rated power. In this case, it is set to the rated power ($P_{rated,i}$) of the device, i.e.:

$$P_i^*(t) = P_{rated,i} \tag{19}$$

Case (1-2): $P_i(t)$ exceeds the remaining storage capacity of device *i*. In this case, the power is injected to the device until the maximum allowable level of the stored energy is reached ($SOC_{\max}$):

$$P_i^*(t) = \frac{P_{rated,i}}{100}(SOC_{\max,i} - SOC_i(t-1)) \tag{20}$$

The value of $SOC_{\max}$ is obtained within the context of the optimization procedure.

Case (1-3): $P_i(t)$ is beyond the HBR. Hence, the power to be drawn from the device does not fall within the allowable range and no power can be delivered, i.e.:

$$P_i^*(t) = 0 \tag{21}$$

Case (1-4): The operating limitations of the device considering its dynamics are not satisfied. For instance, the change in the power share of the device from time step *t* to *t* + 1 is more than the maximum tolerable rate of the power change due to the system inertia (i.e., the power ramp rate, represented by *r*). This inertia implies the impossibility of timely tracking very rapid input power fluctuations [23].

$$P_i^*(t) = r \cdot \Delta t \tag{22}$$

In above mentioned cases, the power assigned to other devices, $P_j(t)$, should also be modified because the constraint did not allow the device *i* to fulfill the storage of its initially assigned $P_i(t)$, calculated in (18). Therefore, a portion of $P_i(t)$ is still remained, namely $P_{rem,i}(t)$, which other devices may be able to absorb it. The modification procedure is named Charge Share Correction (CSC), written as follows:

$$P_{rem,i}(t) = P_i(t) - P_i^*(t) \tag{23}$$

$$CS_i^*(t) = 0 \tag{24}$$

$$CS_j^*(t) = CS_j\left(1 + \frac{CS_i}{\sum_{k=1,k\neq i}^{n} CS_k}\right) \quad \text{for } j \neq i, j = 1, \ldots, n \tag{25}$$

$$P_j^*(t) = P_j(t) + CS_j^*(t) \cdot \sum_{k=1}^{i-1} P_{rem,k}(t) \tag{26}$$

where $CS_j$ is the charge share of all devices except device *i*, and $P_j^*(t)$ is the modified power assumed for the storage device *j*. Eq. (24) means that the device *i* has absorbed all possible amount of power it could, and there is no more power stored in it during the current time step *t*. If one of the constraints corresponding to this device is violated, the same modification procedure is then performed, for that constraint.

For $P_{rem}(t) < 0$: In this case, the load demand is partially supplied by RES. Hence, Discharge Shares (DS) should be determined and assigned to the back-up devices. Utilizing these back-up devices, the effort is made to fully compensate the remaining power by the power from suppliers other than the RES ($P_{backup}$), and try to achieve $P_{backup} = |P_{rem}|$.

The power to be drawn from backup device *i*, $P_i(t)$, is written as follows:

$$P_i(t) = DS_i(k) \cdot P_{rem}(t) \quad i = 1, \ldots, m \tag{27}$$

where *m* is the total number of back-up devices capable of feeding power to the load and $DS_i(k)$ is the discharge share of the back-up device *i* in month *k* (*k* = 1,. . .,12). All *DSs* fall within the range (0,1).

As shown in Fig. 3, the status of all back-up devices is checked one after another considering their constraints and limitations on the power that they are able to serve in the current time step. If any constraint is violated, $P_i(t)$ of the device should be modified, as follows, so that the violated constraint is satisfied.

Case (2-1): $P_i(t)$ exceeds the rated power of device *i*. (Eq. (21) should be applied.)

Case (2-2): The stored energy in the device in the current simulation time step is not as adequate as to supply $P_i(t)$. In this case,

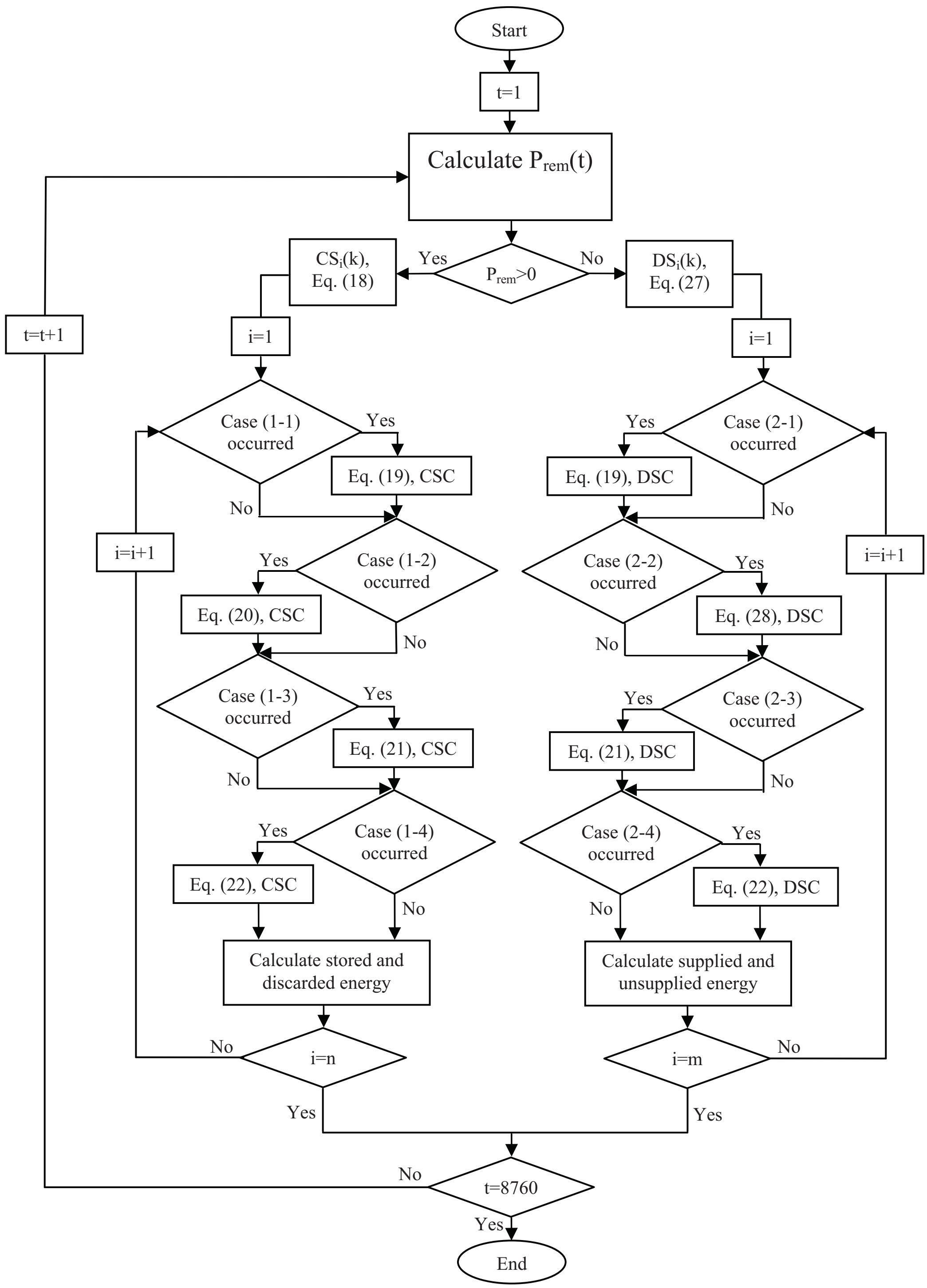



**Fig. 3.** Flowchart of proposed PMS.

the power is drawn from the device until the minimum allowable level of the stored energy is reached ($SOC_{\min,i}$):

$$P_i^*(t) = \frac{P_{rated,i}}{100}(SOC_i(t-1) - SOC_{\min,i}) \tag{28}$$

The value of $SOC_{\min}$ is obtained within the context of the optimization procedure.

Cases (2-3) and (2-4): These cases are the same as cases (1-3) and (1-4), respectively.

In the above mentioned cases, the power assigned to other devices, $P_j(t)$, should also be modified because the constraint did not allow device $i$ to fulfill the supply of its initially assigned $P_i(t)$, calculated in (27), and a portion of $P_i(t)$ is still remained, namely $P_{rem,i}(t)$, which other devices may be able to supply it. The modification procedure is named Discharge Share Correction (DSC), written the same as CSC (Eqs. (23)–(25)), with only replacing all *CS* variables by *DS*, and *n* by *m*.

While any of the above situations take place and CSC or DSC is performed, it is possible that again, the modified dispatch shares are incompatible with system operation constraints. In this case, the CSC or DSC is performed for the second time so that the constraints are satisfied. This is the last effort for the determination of dispatch

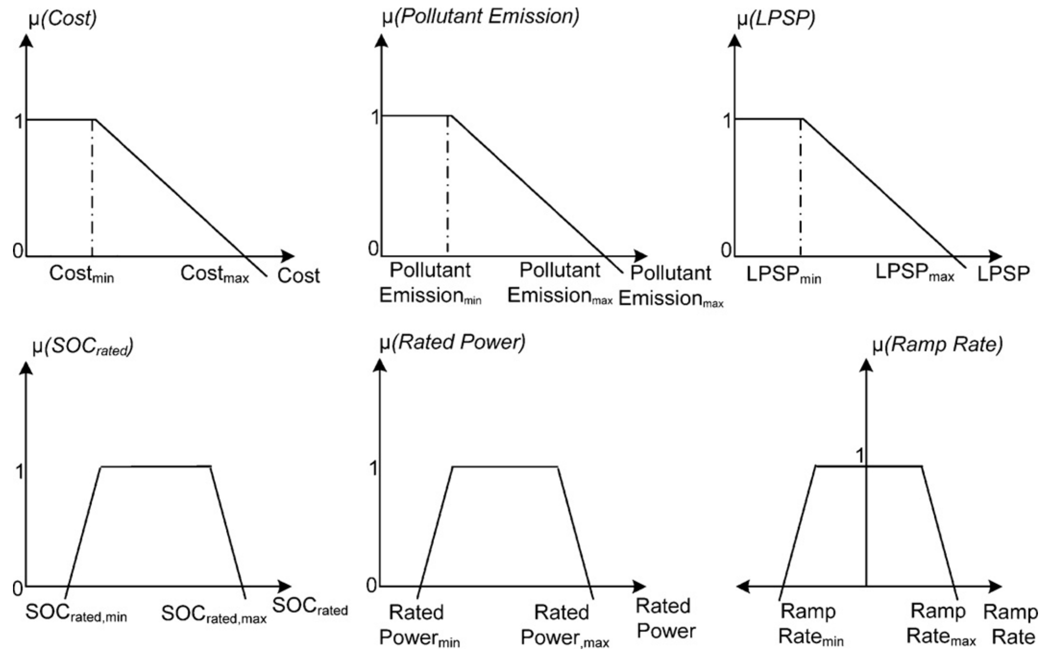



**Fig. 4.** Membership functions of objective functions and constraints.

shares. Then the remaining excess or deficient power is considered as discarded or unmet power in the current simulation time step, respectively (as presented in Fig. 3).

## 4. Optimization algorithm

The multi-objective optimization algorithm proposed in this paper, takes the advantage of the differential evolution algorithm accompanied with fuzzy-multi objective technique.

### 4.1. Multi-objective optimization using fuzzy technique

The multi-objective problem is generally solved by three types of methods. The first one is pareto-based approach to get a set of non-dominated solutions in the process of optimization [24]. The second one is the coefficient method and the last method is transforming the multiple objective function into a single objective model and optimizing it through single objective strategies [24]. In this method, the determination of appropriate values for the coefficients is of very important. In addition, the results are highly dependent on and sensitive to selected values for coefficients. In the method developed by Bellman and Zadeh [25], the single objective problem is achieved by maximizing the minimum degree of satisfaction among membership functions.

The basic idea in fuzzy optimization is to optimize objective function and constraints simultaneously [26]. The fuzzy decision is marked out due to the intersection of fuzzy objectives and fuzzy constraints. The first operation is the fuzzification process of the merged objective function and the constraints. In this procedure, two types of function $\mu(x)$ are defined for each objective function and constraint, as shown in Fig. 4. In this figure, the minimum value for each objective is obtained by the single objective optimization and the maximum value is specified by the initial set of control variables in the optimization algorithm. According to this method, it is possible to change the effectiveness of any objective function by reducing or increasing its specified maximum value. In other words, when the specified maximum value of an objective function decreases, it is considered to be more important in the optimization than the previous state and vice versa. These membership functions are initially combined by “and” operator (minimum). This procedure can be expressed by the following equation:

$$\mu_D(x) = \min(\mu_{f1}(x), \mu_{f2}(x), \ldots, \mu_{c1}(x), \mu_{c2}(x), \ldots) \tag{29}$$

where $\mu_D(x)$ represents the membership function of the optimal decision function and is treated as the evaluation value in the optimization algorithm.

The membership values express the degree of satisfaction for each objective. Highly satisfied objective is given a low value, though lowly satisfied one is assigned a high value. Hence, the multi-objective problem can be transformed into the following maximization problem subject to a crisp constraint set:

$$\max \mu_D(x, u) s.t. \quad H(x, u) = 0, \quad C(x, u) \leq 0 \tag{30}$$

where $\mu_D(x,u)$ is called the fuzzy index.

### 4.2. Differential evolution algorithm

Differential Evolution Algorithm (DEA), introduced by Storn and Price [27], is a simple population based stochastic parallel search evolution algorithm for global optimization and is capable of handling non-differentiable, nonlinear and multi-modal objective functions [28]. In DEA, the population consists of real-valued vectors with dimension $D$, which is equal to the number of control variables. The initial population with the size $Np$, is uniformly distributed in the search space, falling within variables' boundaries. The procedure of this algorithm is shown in Fig. 5. The algorithm is described in the following steps:

**Step (1), Initialization**

For each control variable $k$ with lower bound $x^k_{\min}$ and upper bound $x^k_{\max}$, initial values are randomly and uniformly chosen in the interval $[x^k_{\min}, x^k_{\max}]$:

$$x^k_{i,G} = x^k_{\min} + \text{rand } [0, 1] \times (x^k_{\max} - x^k_{\min}) \quad i \in [1, N_p], \quad k \in [1, D] \tag{31}$$

**Step (2), Evaluation**

In DEA, after generation of the initial population $X_G$, all of its consisting vectors are evaluated by the calculation of the objective function in its subprogram, and then the vectors are sorted according to their objective function value. In the present work, DEA is

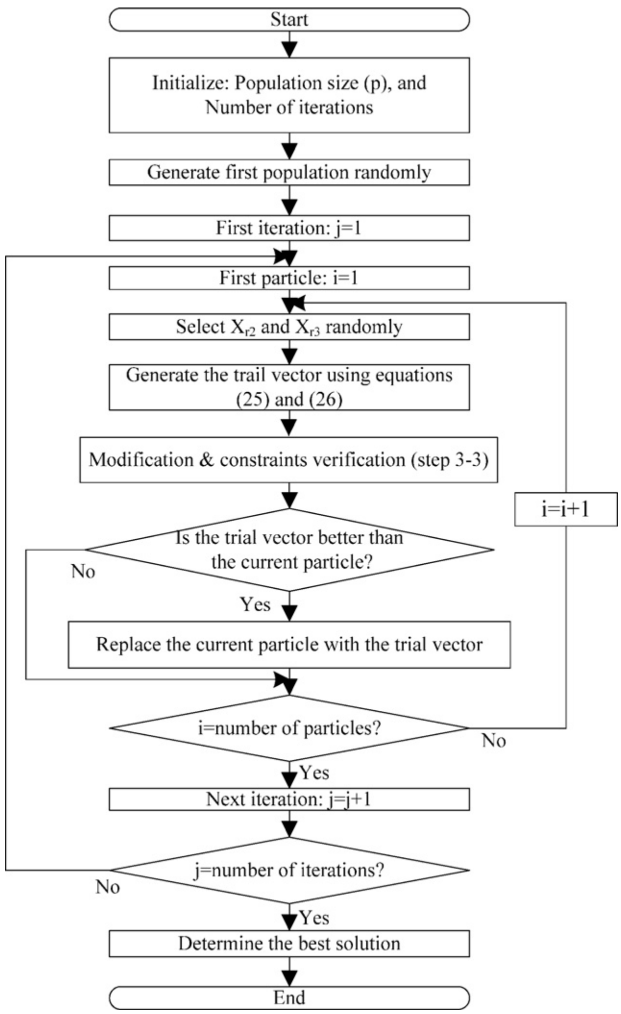



**Fig. 5.** Procedure of the used DEA.

accompanied with fuzzy technique to handle the multi-objective problem. Hence, this step has some differences, described in Section 4.4.

**Step (3), Iteration**

This step is the main procedure of DEA to conduct the final results, which is performed iteratively, until either an acceptable solution has been reached, or for at least a specified number of iterations, no further improvement in the solution is obtained, or a predefined number of iterations are completed [28].

*Step* (3-1), *Mutation*:

In DEA, the perturbations applied to the current population to generate new population are derived from the current population itself, and no predefined probability density function is considered. For a given vector of control variables, $X_{i,G}$, in the population, two vectors ($X_{r_2,G}$ and $X_{r_s,G}$) are randomly selected such that the indices $i$, $r_2$ and $r_3$ are mutually different. Then, the weighted difference between two vectors is added to the vector with the best fitness function, $X_{b,G}$, written as follows:

$$V_{i,G+1} = X_{b,G} + F \cdot (X_{r_2,G} - X_{r_3,G}) \quad r_2, r_3 \in \{1, 2, \ldots, N_P\} \tag{32}$$

where $F$, a constant from (0, 2), characterizes the amount of the movement of vectors within the search space.

*Step* (3-2), *Crossover*:

In this step, the trial vector $U_{i,G+1}$ is developed from the elements of the target vector $X_{i,G}$ and the elements of the mutant vector $V_{i,G+1}$. The elements of the mutant vector enter the trial vector with probability $CR$ as follows:

$$U_{j,i,G+1} = \begin{cases} V_{j,i,G+1} & \text{if } \text{rand}_{j,i} \le CR \text{ or } j = I_{\text{rand}} \\ X_{j,i,G} & \text{if } \text{rand}_{j,i} > CR \text{ and } j \ne I_{\text{rand}} \end{cases} \tag{33}$$

where $\text{rand}_{j,i} \in [0,1]$, $I_{\text{rand}}$ is an integer randomly selected from [1,2,..., $D$]. $I_{\text{rand}}$ ensures that one of the trial vectors is selected among the mutant vectors.

*Step* (3-3), *Modification and constraints verification*:

This step prepares the trial vectors for the next step by verifying the variables whether they meet their constraints, given in Sections 3.2 and 4.4. Otherwise, for the vectors containing variables with unsatisfied constraints, mutation and crossover steps are repeated for a specified number of times or until the problem is fixed. Nevertheless, these vectors will be regenerated, similar to step (1).

*Step* (3-4), *Selection*:

The vectors generated in the previous step are evaluated and sorted as described in the step (2). Then, the trial vector $U_{i,G+1}$ is compared with the corresponding vector $X_{i,G}$ and the one with the better fitness value is admitted to the next iteration as $X_{i,G+1}$:

$$X_{i,G+1} = \begin{cases} U_{i,G+1} & \text{if} f(U_{i,G+1}) < f(X_{i,G}) \\ X_{i,G} & \text{otherwise} \end{cases} \quad i \in [1, N_P] \tag{34}$$

### 4.3. Representation of uncertainty

Natural characteristics of wind and solar energy impose uncertainty in their design and operation. Hence, considering various possible scenarios in the model of these resources can lead to more realistic decisions. The uncertain parameters are expressed by probability distributions, showing the range of values that a parameter could take, and also accounting for the probability of the occurrence of each value in the considered range [12]. In this paper, Weibull and Beta PDFs are used for the wind speed and the solar irradiation, respectively [21]. Using this solution, seven scenarios are generated, to model the uncertainty of these resources.

### 4.4. Implementation

A program in MATLAB environment is developed to determine the best set of design and PMS parameters. Furthermore, the convergence and computational time for the algorithm is evaluated. The same system is simulated via two other optimization methods widely applied to renewable energy [29], namely Genetic Algorithm (GA) [30] and Linearly Decreasing Inertia Particle Swarm Optimization (LDI-PSO) [31,32] and their corresponding results are compared in the Section 5.2. The performance of the proposed PMS is also evaluated by comparison with another PMS.

There are two main modules in the developed program, the optimization module and the system simulation module. The first module generates and modifies a valid vector of control variables to be evaluated by the system simulation module in each iteration. When the latter module is invoked, the input vector is processed. The module simulates the operation of the system for each scenario, calculates the operating point of each system component and determines $\mu_{f,i}(x)$ and $\mu_{ci}(x)$, and the resultant $\mu_D(x)$, using the resultant values for objective functions. These values are transformed into a single value using the described fuzzy technique and become the evaluation value for the considered scenario. The final evaluation value for an input vector is the average of values obtained by using data of all generated scenarios [12], which is then admitted back to the optimization module.

Therefore, a valid control vector is obtained by assigning values to the control variables that lie within allowed bounds of each

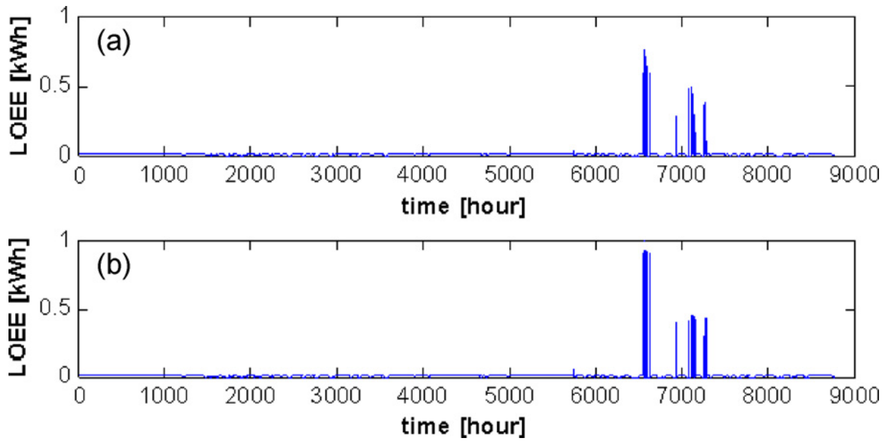



**Fig. 6.** LOEE for (a) PMS (a) and (b) PMS (b).

individual. However, some modifications to the original optimization algorithm are made to match the specific characteristics of the present problem, as follows:

- Some of the control variables, including number and type of each component, must be non-negative integers. Therefore, the optimization procedure should handle the discrete variables in all initialization, crossover and mutation steps.
- The upper limit, associated with $CS_i$ and $DS_i$ ($i$ = 2,. . .,$n$) float in accordance with the values of $CS_k$ and $DS_k$ ($k$ = 1,. . .,$i$ − 1), because $CS_i$ and $DS_i$ must satisfy the equality constraint $\sum_{k=1}^{n} CS_k = \sum_{k=1}^{m} DS_k = 1$. This constraint modification is applied to the value that the optimization procedure assign to $CS_i$ and $DS_i$, from device $i$ = 1 through $n$, one by one, i.e.:

$$CS_1^{\max} = 1, \qquad CS_i^{\max} = 1 - \sum_{k=1}^{i-1} CS_k \quad (i = 2, \ldots, n) \tag{35}$$

  A similar equation is used by replacing $CS$ by $DS$ and $n$ by $m$.
- The integration of the fuzzy model with the optimization procedure for handling the multi-objective problem consists of developing membership functions of objectives as well as constraints imposed on the operation of the system. By solving a single objective optimization for each objective function, its minimum and maximum values are obtained and the corresponding membership function is achieved. By the way, using maximum and minimum power ramp rates of each component ($ramp\ rate_{i,\min}$ and $ramp\ rate_{i,\max}$), rated limitations on $SOC_i$ ($SOC_{i,\min}$ and $SOC_{i,\max}$) and power boundaries of each component ($rated\ power_{i,\min}$ and $rated\ power_{i,\max}$), all as the operation constraints, their corresponding membership functions are obtained (as shown in Fig. 4).
- To treat the uncertain parameters, several scenarios are generated and simulated. Hence, all the three objective functions introduced in Section 3.1 are calculated for all the scenarios. The algorithm utilizes the concept of the "expected objective function", which aggregates all the objective function values corresponding to the simulated scenarios representing the uncertain parameters, in the form of an average value [12]. Then, using the expected objective function values, the fuzzy index is calculated, and the algorithm continues with the same algorithmic operations found in DEA. In this way, the results represent the solution with an overall consideration of all scenarios associated with the uncertain parameters in the system.

## 5. Case study and results

### 5.1. System data

The hybrid energy system under study has been described in Section 2. In practical system planning, the designer has to choose the system components from a set of commercially available ones. As a case study, various models and types of components with different rated powers, costs and other specification [15], are the input to the design procedure. The system location is a region in Ardebil city (38°14′57″N/48°18′5″E), in the north west of Iran. For this region, the hourly data for solar irradiance, wind speed and ambient temperature all provided within one year period [2]. The considered load profile is the IEEE reliability test system [33] with 30 kW peak power.

### 5.2. Results

The data are analyzed to determine the optimum design and PMS parameters for the case study. The results of the used optimization algorithms, i.e., GA, LDI-PSO and DEA, are presented in Table 1. It can be seen in this table that DEA revealed the best performance with respect to optimization of objective functions and the resultant fuzzy index. Hence, DEA is nominated to demonstrate the results of this problem in more detail. Since, this problem should be solved in off-line mode, the computation time and convergence speed are not of great concern.

In order to well present the applicability and efficacy of the proposed PMS, which is the significant idea of this paper, a simulation is also carried out by using another PMS, referred to as PMS (b). Based on the PMS (b) which is analogous with the PMS (dispatch strategy) employed in the HOMER software [8], $P_{rem}(t)$ in time step $t$ is dispatched among components by the priorities defined by designer, unless the marginal cost of energy storage or production of the dispatched power by the components is in contrast with

**Table 1**
Results of three evolutionary algorithms.

| | PMS (a) | | | PMS (b) |
|---|---|---|---|---|
| | GA | LDI-PSO | DEA | DEA |
| Cost (€) | 1,042,242 | 967,375 | 912,560 | 918,337 |
| Fuel emissions (kg) | 2086.2 | 2632.8 | 1827.7 | 2888.6 |
| $LPSP$ (W/h) | 0.0067 | 0.0083 | 0.0072 | 0.0075 |
| Number of iterations to converge | 29550 | 196 | 227 | 153 |
| Computation time (s) | 173,520 | 121,311 | 134,548 | 72,549 |
| Fuzzy index | 0.9980 | 0.9973 | 0.9996 | 0.9915 |

**Table 2**
Optimized values for design parameters of the case study.

| Design data | | DEA |
|---|---|---|
| **Equipments data** | | |
| PV panel | Number | 9 |
| | Type | 10 |
| Wind turbine | Number | 6 |
| | Type | 6 |
| Battery | Number | 28 |
| | Type | 5 |
| Fuel cell | Number | 6 |
| | Type | 4 |
| Electrolyzer | Number | 8 |
| | Type | 4 |
| Diesel generator | Number | 7 |
| | Type | 3 |
| Hydrogen tank | Number | 6 |
| Inverter nominal power (kVA) | Type | 35 |
| **Installation data** | | |
| Wind tower height (m) | | 32 |
| PV panels monthly tilt angle $\beta_1 - \beta_{12}$ (°) | | 67 |
| | | 58 |
| | | 63 |
| | | 46 |
| | | 38 |
| | | 31 |
| | | 22 |
| | | 30 |
| | | 26 |
| | | 43 |
| | | 59 |
| | | 53 |

the predefined priorities. In this case, the priority of components to store or produce $P_{rem}(t)$ is sorted ascendingly according to their corresponding cost of energy storage or production. The optimization results using PMS (b) are included in Table 1, too. It can be observed that PMS (a) have better results than PMS (b). The fuel emission is comparably less than that of PMS (b), showing that the utilization of back-up and storage devices other than the diesel generator is more effective when PMS (a) is employed. Fig. 6 presents the *LOEE* in both PMS cases, confirming the better *LPSP* of Table 1 for the case of PMS (a).

Table 2 presents the result of design parameters, including the type and number of each component. The installation data consisting of the monthly PV panels tilt angle and wind turbines installation height are also listed in the table.

The monthly values of charge and discharge shares are presented in Figs. 7 and 8, respectively. Fig. 7 presents that the *DS* of fuel cells is more significant in winter's months than summer's months and the opposite is true for diesel generators. The values obtained for *DS* parameters also have great influence on the *CS*

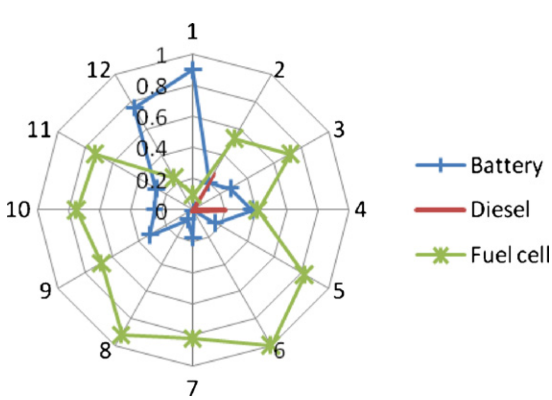



**Fig. 7.** Monthly dispatch shares of backup devices for providing the deficient demand.

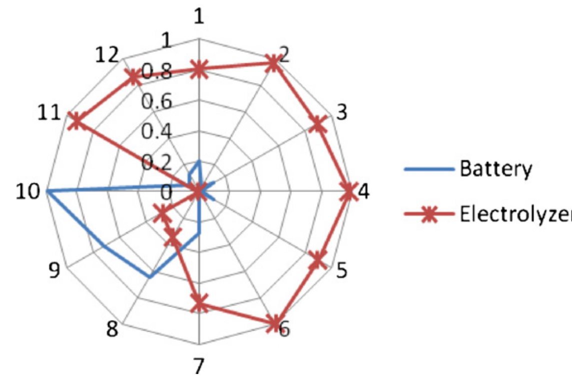



**Fig. 8.** Monthly dispatch shares storage devices for saving the excess power.

**Table 3**
Optimized values of limitations of storage devices.

| Storage device limitations | DEA |
|---|---|
| Minimum state of charge of batteries ($SOC_{min}$ %) | 21 |
| Maximum state of charge of batteries ($SOC_{max}$ %) | 100 |
| Minimum level of Hydrogen in tanks (%) | 33 |

values. In fact, *CS* and *DS* parameters are interdependent for components that utilize the same energy storage device in both charging and discharging states. For instance, electrolyzers and fuel cells use the same energy container namely hydrogen tanks to store energy and consume it, respectively. Table 3 contains optimized values of operating limitations of storage devices.

The attained values for parameters of PMS by represent nearly the overall optimum operating condition of the system considering a compromise among all the considered objectives. The parameters are separately calculated for each month, representing the influence of monthly and seasonal changes in load demand and climatic patterns on the utilization of the hybrid system. Hence, the results are adapted with any circumstances that alter the operation of the system resulting in more accuracy and optimality.

## 6. Conclusions

This study has been dedicated to review optimal design and operation strategy selection of hybrid RES-based stand-alone energy systems, including various generators and storage media. Considering resource uncertainties, associated with wind speed and solar irradiation, a novel method has been proposed, to determine the power management strategy of the system along with sizing parameters of system components so that the overall cost of the system during its useful lifetime, unmet load and pollutant emissions have been minimized. The PMS parameters are monthly charge shares (*CS*) of storage devices and monthly discharge shares (*DS*) of generator devices, limitations on their start-up/shut-down power thresholds (HBR) and on their level of available energy (SOC).

Based on the proposed method, the values of PMS parameters, the sizing and design parameters have been determined by the iterative optimization algorithm. The PMS parameters have been separately determined for each month to adapt monthly variations in the load and climate patterns. Then in each iteration, these values have been applied to the hourly simulation of the system operation and evaluated in each single time step to meet the operational constraints of the components, consisting of the nominal power, $SOC_{min}$ and $SOC_{max}$, HBR, and power ramp rate of each device. Otherwise, these values have been modified by either of two operators, namely CSC or DSC, in that time step. These modifications have ensured that while the optimum operation strategy and commitment of components has been attained, all constraints associated

with operational characteristics of the components have been satisfied. However, if after completion of all steps of simulation in a time step, the constraints were still unsatisfied, some discarded or unsupplied energy remains. The summation of these values during all time steps of the simulation has been involved in the objective functions to be minimized.

The proposed method has tested on a hybrid PV–wind–diesel–hydrogen–battery system. To efficiently handle the nonlinear mixed-integer multi-objective optimization problem, a modified version of DEA accompanied by fuzzy technique has implemented. The system has been optimized for summations of all objective values of each function calculated for all scenarios generated by applied uncertainty models. The presented results of the solution can be categorized into three groups:

- Size (design) data: The optimum number and type of each component of the system to be installed.
- Installation data: The optimum values for monthly inclination angles of solar panels and the optimum tower height for wind turbines installation to maximize the exploitable power from RES.
- Operation strategy (PMS): The monthly *CS* and *DS*, and boundaries associated with SOC.

By comparing the results of design parameters and objective functions values (accompanied by that of the system operation and unsupplied energy), with the results of applying a user-defined PMS, it has been concluded that the design decisions and operation of such systems are highly affected by the employed PMS; and the superiority of the proposed PMS has been confirmed. It should be mentioned that the proposed method can be effectively employed for any composition of hybrid energy systems.

## References


[1] Shahnia F, Majumder R, Ghosh A, Ledwich G, Zare F. Operation and control of a hybrid microgrid containing unbalanced and nonlinear loads. Electric Power Systems Research 2010;80:954–65.

[2] Kashefi Kaviani A, Riahy G, Kouhsari S. Optimal design of a reliable hydrogen-based stand-alone wind/PV generating system, considering component outages. Renewable Energy 2009;34:2380–90.

[3] Nelson D, Nehrir M, Wang C. Unit sizing and cost analysis of stand-alone hybrid wind/PV/fuel cell power generation systems. Renewable Energy 2006;31:1641–56.

[4] Seeling-Hochmuth G. A combined optimisation concet for the design and operation strategy of hybrid-PV energy systems* 1. Solar Energy 1997;61: 77–87.

[5] Muselli M, Notton G, Louche A. Design of hybrid-photovoltaic power generator, with optimization of energy management. Solar Energy 1999;65: 143–57.

[6] Koutroulis E, Kolokotsa D, Potirakis A, Kalaitzakis K. Methodology for optimal sizing of stand-alone photovoltaic/wind-generator systems using genetic algorithms. Solar Energy 2006;80:1072–88.

[7] Maghraby H, Shwehdi M, Al-Bassam GK. Probabilistic assessment of photovoltaic (PV) generation systems. IEEE Transactions on Power Systems 2002;17:205–8.

[8] Dufo-López R, Bernal-Agustín JL. Design and control strategies of PV-Diesel systems using genetic algorithms. Solar Energy 2005;79:33–46.

[9] Mohamed FA, Koivo HN. System modelling and online optimal management of MicroGrid using mesh adaptive direct search. International Journal of Electrical Power & Energy Systems 2010;32:398–407.

[10] Garcia RS, Weisser D. A wind–diesel system with hydrogen storage: joint optimisation of design and dispatch. Renewable Energy 2006;31:2296–320.

[11] Bernal-Agustín JL, Dufo-Lopez R. Multi-objective design and control of hybrid systems minimizing costs and unmet load. Electric Power Systems Research 2009;79:170–80.

[12] Giannakoudis G, Papadopoulos AI, Seferlis P, Voutetakis S. Optimum design and operation under uncertainty of power systems using renewable energy sources and hydrogen storage. International Journal of Hydrogen Energy 2010;35:872–91.

[13] Ierapetritou M, Acevedo J, Pistikopoulos E. An optimization approach for process engineering problems under uncertainty. Computers & Chemical Engineering 1996;20:703–9.

[14] Dufo-López R, Bernal-Agustín JL, Contreras J. Optimization of control strategies for stand-alone renewable energy systems with hydrogen storage. Renewable Energy 2007;32:1102–26.

[15] Dufo-Lopez R, Bernal-Agustin JL. Multi-objective design of PV–wind–diesel–hydrogen–battery systems. Renewable Energy 2008;33:2559–72.

[16] Mondol JD, Yohanis YG, Norton B. The impact of array inclination and orientation on the performance of a grid-connected photovoltaic system. Renewable Energy 2007;32:118–40.

[17] Chang YP. Optimal the tilt angles for photovoltaic modules in Taiwan. International Journal of Electrical Power & Energy Systems 2010;32:956–64.

[18] Zghal W, Kantchev G, Kchaou H. Optimization and management of the energy produced by a wind energizing system. Renewable and Sustainable Energy Reviews 2011;15:1080–8.

[19] Hybrid optimization model for electric renewables (HOMER). wwwnrelgov/international/homer.

[20] Mostafaeipour A, Sedaghat A, Dehghan-Niri A, Kalantar V. Wind energy feasibility study for city of Shahrbabak in Iran. Renewable and Sustainable Energy Reviews 2011;15:2545–56.

[21] Atwa Y, El-Saadany E, Salama M, Seethapathy R. Optimal renewable resources mix for distribution system energy loss minimization. IEEE Transactions on Power Systems 2010;25:360–70.

[22] Bagul A, Salameh Z, Borowy B. Sizing of a stand-alone hybrid wind–photovoltaic system using a three-event probability density approximation. Solar Energy 1996;56:323–35.

[23] Auld AE, Samuelsen S, Brouwer J, Smedley K. Load-following strategies for evolution of solid oxide fuel cells into model citizens of the grid. IEEE Transactions on Energy Conversion 2009;24:617–25.

[24] Zhang W, Liu Y. Multi-objective reactive power and voltage control based on fuzzy optimization strategy and fuzzy adaptive particle swarm. International Journal of Electrical Power & Energy Systems 2008;30:525–32.

[25] Bellman RE, Zadeh LA. Decision-making in a fuzzy environment. Management Science 1970:B17–41.

[26] Baer B, Butler K, Hiyama T, Kubokawa J, Lee K, Luh P, et al. Tutorial on fuzzy logic applications in power systems; 2000.

[27] Storn R, Price K. Differential evolution – a simple and efficient heuristic for global optimization over continuous spaces. Journal of Global Optimization 1997;11:341–59.

[28] Varadarajan M, Swarup K. Differential evolutionary algorithm for optimal reactive power dispatch. International Journal of Electrical Power & Energy Systems 2008;30:435–41.

[29] Ba os R, Manzano-Agugliaro F, Montoya F, Gil C, Alcayde A, Gómez J. Optimization methods applied to renewable and sustainable energy: a review. Renewable and Sustainable Energy Reviews 2011;15:1753–66.

[30] Elbeltagi E, Hegazy T, Grierson D. Comparison among five evolutionary-based optimization algorithms. Advanced Engineering Informatics 2005;19: 43–53.

[31] del Valle Y, Venayagamoorthy GK, Mohagheghi S, Hernandez JC, Harley RG. Particle swarm optimization: basic concepts, variants and applications in power systems. IEEE Transactions on Evolutionary Computation 2008;12: 171–95.

[32] Shi Y, Eberhart R. A modified particle swarm optimizer. IEEE 1998:69–73.

[33] IEEE Reliability Test System. http://wwweewashingtonedu/research/pstca/rts/pg_tcartshtm.